Journal of Alloys and Compounds, 191 (1993) 127–130
JALCOM 490

Role of the heating rate up to the annealing temperature on the hysteretic properties of hard magnetic materials prepared from amorphous precursors

V. E. Martín[a], J. Bernardi[b], J. Fidler[b], F. Cebollada[a] and J. M. González[a,*]
[a]*Instituto de Ciencia de Materiales, CSIC, c/ Serrano 144, E-28006 Madrid (Spain)*
[b]*Institute of Applied and Technical Physics, TU Vienna, Wiedner Hauptst. 8–10, A-1040 Vienna (Austria)*

(Received August 17, 1992)

Abstract

Data are presented on the influence of the heating rate up to the treatment temperature used during the crystallization of amorphous precursors of hard samples on the parameters characterizing their final demagnetization process. The results can be directly correlated to the microstructural features observed in the samples. It is concluded that the precipitation of deteriorating phases (α-Fe) can be avoided by using sufficiently high heating rates, which demonstrates the relevance of this parameter.

1. Introduction

Although suitable values of some intrinsic properties, *e.g.* magnetocrystalline anisotropy, saturation magnetization and order temperature, are fundamental requisites in order to develop magnetic hardness, the hysteretic behaviour is ultimately determined by the particular features of the microstructure of the materials [1]. Because of this, the use of amorphous or metastable precursor phases in the preparation of permanent magnet materials is a very promising route since it makes possible, to a very large extent, the formation of highly homogeneous microstructures, the tailoring of some important parameters, *e.g.* mean grain size, and the production of a structure of secondary phases different from that obtained using conventional techniques [2, 3].

Regarding the investigation of this preparation strategy, it is worth pointing out that the crystallization of an amorphous phase in an approach-to-equilibrium process that should be clearly distinguished from the regular equilibrium phase transformations. Therefore, from a thermodynamic point of view, the crystallization processes are only described when kinetic information similar to that contained in the time–temperature–transformation curves is given [4]. However, even if these curves are known, in the usual case of a process which follows additive kinetics, the basic characteristics of the microstructure of the crystallization product will require an additional, independent study. This is related to the fact that the crystallization rate results from a convolution of the nucleation and growth rates, which depend in different ways on the temperature [5]. For systems far from equilibrium, both mechanisms follow an Arrhenius behaviour, and if the activation energy for the growth mechanism is lower than that for nucleation, growth will govern the crystallization for lower temperature treatments whereas nucleation will predominate at higher temperature.

As a direct consequence of this, a wide range of microstructures can be accessed when crystallizing amorphous precursors of hard magnetic materials, thus giving rise to the possibility of optimizing their extrinsic magnetic properties. Examples of this for the NdFeB and NdDyFeB systems, have been reported previously in refs. 2 and 3, where data on the characteristics of the crystallization process, the basic microstructural features and the influence on the hysteretic parameters of the temperature and time of thermal treatment were presented.

In this work we study the influence of the heating rate up to the treatment temperature on the demagnetization process of the crystallized material. Our magnetic measurements will be correlated with the results of a detailed microstructural characterization of the samples in order to make evident the relevance of this parameter in the achievement of optimized properties.

*Author to whom correspondence should be addressed.

0925-8388/93/$6.00

2. Sample preparation and experimental methods

The study was carried out on samples of nominal compositions $Nd_9Dy_6Fe_{76}B_9$ and $Nd_9Dy_6Fe_{76}B_9$ obtained by melt spinning (with the wheel rotating at a tangential speed of 30 m s^{-1}). The "as-quenched" samples, in the shape of irregular flakes, were free from crystallites within the resolution of the X-ray diffractometry (XRD), although the measurement of the demagnetization curves of some flakes revealed the presence of a small fraction of hard magnetic phases (always corresponding to less than 10% of the total saturation magnetic moment of the samples).

The basic characterization of the crystallization processes was carried out by means of differential scanning calorimetry (DSC). Continuous heating scans carried out at 20 °C min^{-1} showed that crystallization proceeds by means of a single exothermic process that takes place at 605 and 625 °C for the $Nd_9Dy_6Fe_{76}B_9$ and $Nd_6Dy_9Fe_{76}B_9$ samples respectively.

The phase distribution of the crystallized samples was analysed by means of XRD and their microstructure was studied using scanning and transmission electron microscopies (SEM and TEM). The parameters describing the hysteretic behaviour were measured with an extraction magnetometer based in a 12 T superconducting coil.

3. Experimental results

3.1. Magnetic characterization

We should remark first that all the fully crystallized samples were isotropic within the resolution of our magnetometer. Consequently, owing to the occurrence of large reversible magnetization variations, we decided to distinguish between the demagnetizing field (H_{crit}) for which a maximum in the susceptibility was observed and the field ($H_{M=0}$) which nulls the remanent magnetization. H_{crit} can be identified with the field producing the largest irreversible processes in the main hard magnetic phase (and therefore is equivalent to the coercive force of oriented magnets), whereas $H_{M=0}$ depends for instance on the amount of secondary phases. H_{crit} and $H_{M=0}$ should have the same value in a perfectly oriented single-phase material.

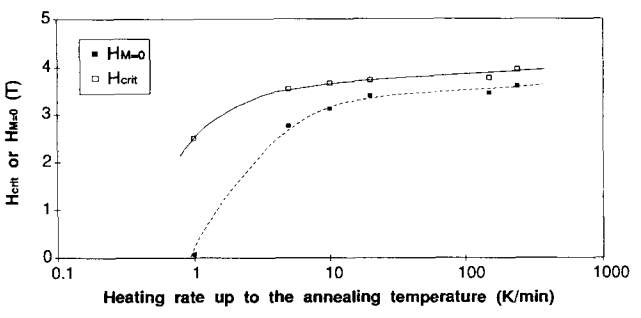

Fig. 1. Dependence of H_{crit} and $H_{M=0}$ on the heating rate in $Nd_9Dy_6Fe_{76}B_9$ samples treated at $T_{ann}=725$ °C for 5 min.

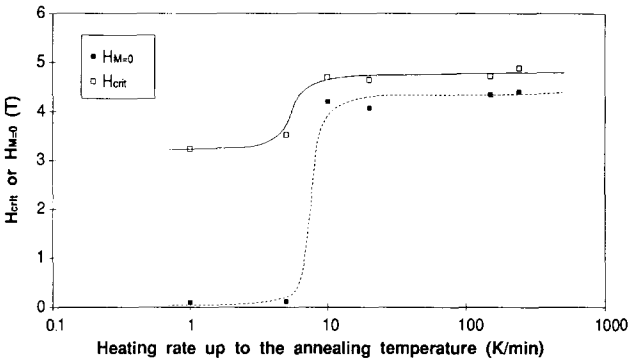

Fig. 2. Dependence of H_{crit} and $H_{M=0}$ on the heating rate in $Nd_6Dy_9Fe_{76}B_9$ samples treated at $T_{ann}=750$ °C for 5 min.

Both parameters were measured in samples thermally treated at $T_{ann}=725$ °C ($Nd_9Dy_6Fe_{76}B_9$) and $T_{ann}=750$ °C ($Nd_6Dy_9Fe_{76}B_9$) for $t_{ann}=5$ min. The treatment temperatures were chosen according to a previous result [3] which indicates that maximum values for H_{crit} are obtained when crystallization takes place at temperatures 100–150 °C above the temperature of the exothermic process observed by DSC while heating the samples at 20 °C min^{-1}. These treatments were repeated using different heating rates r_{ann} ranging from 1 to 240 °C min^{-1}. In Figs. 1 and 2 we present the values (corresponding respectively to $Nd_9Dy_6Fe_{76}B_9$ and $Nd_6Dy_9Fe_{76}B_9$ samples) of H_{crit} and $H_{M=0}$ plotted against the heating rate employed in order to reach T_{ann}. The same qualitative behaviour can be observed in both samples: a slight increase in H_{crit} with increasing heating rate, but a markedly larger increase in $H_{M=0}$. In particular, there exists a large difference between the two parameters when the samples are crystallized using heating rates up to T_{ann} below 10 °C min^{-1}, this difference becoming smaller as the rate of heating reaches the value 100 °C min^{-1}.

3.2. Microstructural characterization

In Fig. 3 we present an SEM image of a fresh fracture surface of an $Nd_6Dy_9Fe_{76}B_9$ sample ($r_{ann}=10$ °C min^{-1}) where the homogeneity of the microstructure of the crystallization product can be observed. This was a general characteristic of the samples studied, the only exception being those treated using the lowest values of r_{ann}, in which a coarser and less homogeneous microstructure was formed (see Fig. 4, where an SEM image corresponding to an $Nd_6Dy_9Fe_{76}B_9$ sample crystallized using $r_{ann}=1$ °C min^{-1} is shown).

In Figs. 5–7 we present TEM images of samples of composition $Nd_6Dy_9Fe_{76}B_9$ heated to the treatment

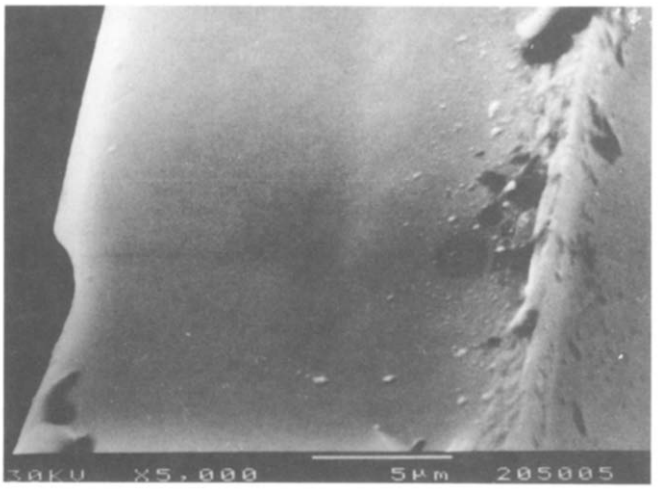

Fig. 3. SEM image of a fresh fracture surface of an $Nd_6Dy_9Fe_{76}B_9$ sample ($r_{ann} \approx 10$ °C min^{-1}).

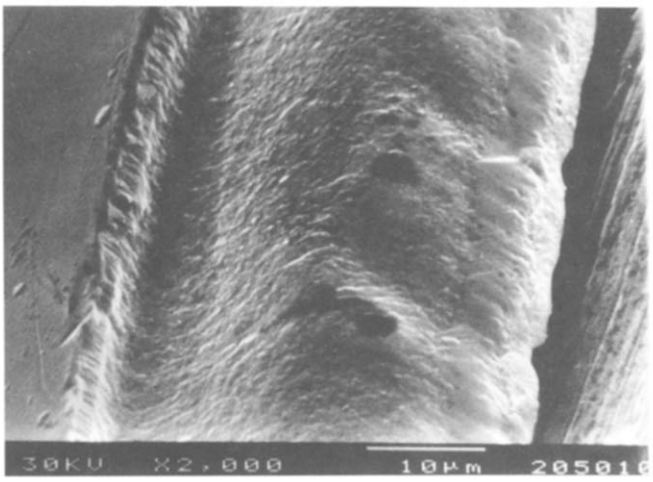

Fig. 4. SEM image of a fresh fracture surface of an $Nd_9Dy_6Fe_{76}B_9$ sample ($r_{ann} = 1$ °C min^{-1}).

temperature at 1, 10 and 240 °C min^{-1} respectively. In the sample corresponding to $r_{ann} = 1$ °C min^{-1} (Figs. 5(a) and 5(b)), large polyhedral grains of sizes up to several tenths of a micrometre (which could be the result of the growth of pre-existing nuclei, favoured by the long time of treatment) as well a much finer microstructure resembling that observed in eutectic decompositions can be observed. Regarding this last feature, we should remember that the nominal compositions we have used do not correspond to the stoichiometry of the 2:14:1 phase and consequently a mix of phases is to be expected if the samples are allowed to reach their lower energy equilibrium phase distribution. The XRD study of these samples annealed at 1 °C min^{-1} showed that a large amount of a phase which could be identified as α-Fe or Fe_2B was present, it being possible to avoid its presence by employing higher heating rates (Fig. 8). The micrographs of Figs.

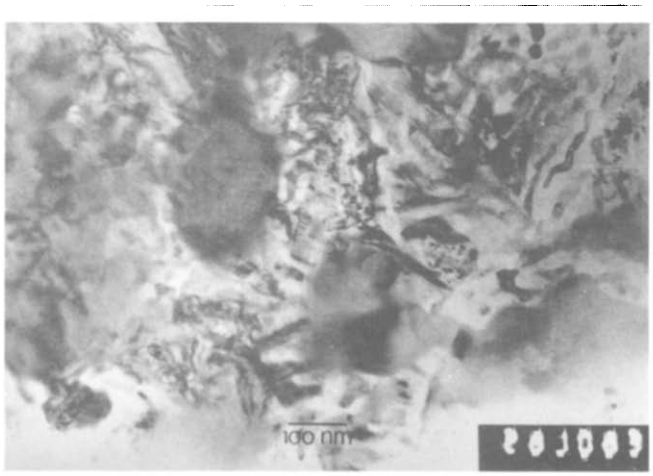

(a)

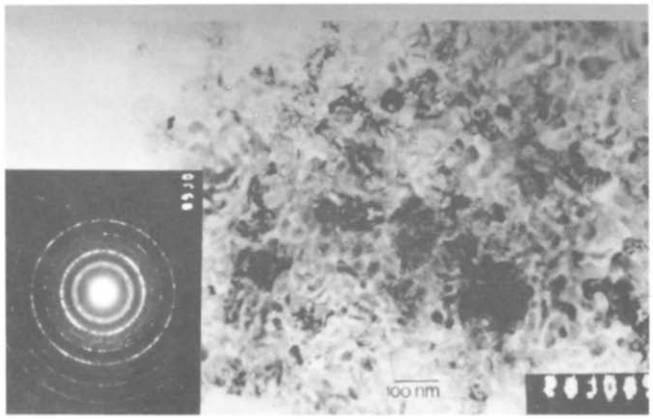

(b)

Fig. 5. TEM images of an $Nd_6Dy_9Fe_{76}B_9$ sample heated to the annealing temperature at 1 °C min^{-1}.

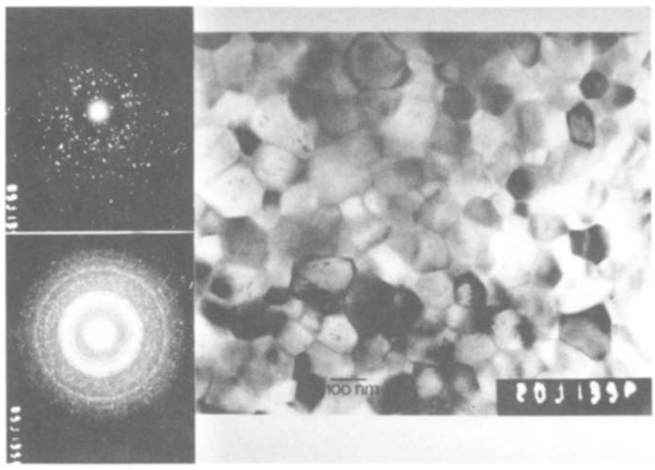

Fig. 6. TEM image of an $Nd_6Dy_9Fe_{76}B_9$ sample heated to the annealing temperature at 10 °C min^{-1}.

6 and 7, corresponding respectively to $r_{ann} = 10$ and 240 °C min^{-1}, show that highly homogeneous microstructures consisting of more or less spherical grains with a mean diameter of 100 nm are formed in these cases.

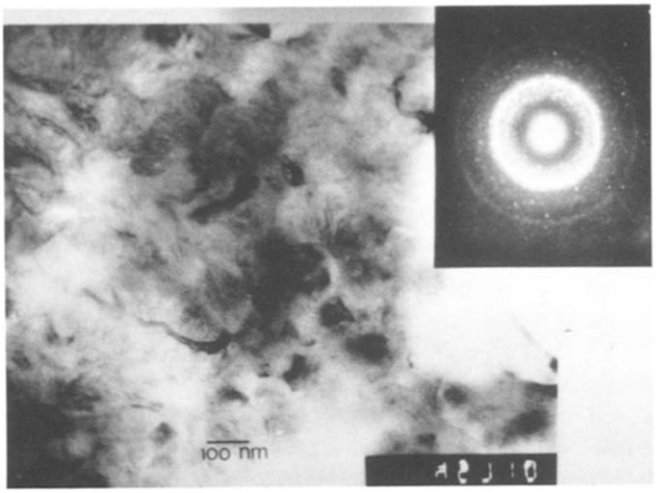

Fig. 7. TEM image of an $Nd_6Dy_9Fe_{76}B_9$ sample heated to the annealing temperature at 240 °C min^{-1}.

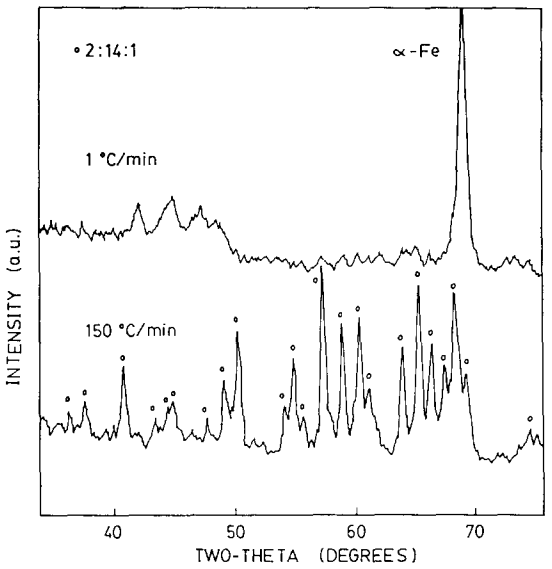

Fig. 8. X-ray diffraction pattern of $Nd_6Dy_9Fe_{76}B_9$ heated to the annealing temperature at $r_{ann}=1$ and 150 °C min^{-1}.

4. Discussion

The relevance of the heating rate up to the treatment temperature used when crystallizing amorphous precursors of hard magnetic materials is evident if we consider that this approach-to-equilibrium process can only be described in kinetic terms.

In addition to this, our results clearly show that this parameter influences to a large extent, through its influence on the microstructure, the hysteretic properties of the final material, allowing us to obtain, by means of a treatment favouring nucleation mechanisms over grain growth, homogeneous microstructures with small rounded grains of the hard phase where demagnetization processes can be confined to the intragrain scale and easy nucleation centres such as sharp edges do not exist.

More importantly, we have shown that, in the samples we have studied, low heating rates should be avoided in order to prevent the segregation of soft phases, this fact being of crucial interest from the point of view of the optimization of the material. This behaviour can be understood by considering that, although our DSC results show a single exothermic peak, both the microstructural studies and the magnetic measurements demonstrate that in addition to the formation of the main 2:14:1 phase α-Fe crystallites may appear owing to the inhomogeneities that are present in the amorphous precursors. In relation to this, the different activation energies of the nucleation and growth mechanisms that are responsible for the formation of each phase allow the possibility of avoiding the presence of significant amounts of soft phases.

References

1 H. Kronmüller and K.-D. Durst, in I. V. Mitchell, J. M. D. Coey, D. Givord and I. R. Harris (eds.), *Concerted European Action on Magnets (CEAM)*, Elsevier, London, 1989, p. 392.
2 M. T. Clavaguera-Mora, J. A. Diego, M. D. Baró, S. Suriñach, N. Clavaguera, J. M. González and F. Cebollada, *J. Alloys Compounds, 182* (1992) 211.
3 J. M. González, F. Cebollada, V. E. Martín, M. Pulido, A. Hernando, E. Pulido and P. Crespo, *J. Magn. Magn. Mater., 104–107* (1992) 1179.
4 U. Köster and H. Herald, in H. Guntherodt and H. Beck (eds.), *Glassy Metals I*, Springer, Berlin, 1981, p. 225.
5 S. Suriñach, M. D. Baró, J. A. Diego, N. Clavaguera and M. T. Clavaguera-Mora, *Acta Metall. Mater., 40* (1992) 37.